Schweizerische Eidgenossenschaft
Confédération suisse
Confederazione Svizzera
Confederaziun svizra

Department of the Environment, Transport, Energy and Communication DETEC

Swiss Federal Office of Energy SFOE
Energy Research

Final report: August 2018

GELSEC – Towards mass production of aerogels through ambient pressure drying

Figure: Polymer reinforced silica aerogels

Empa
Materials Science and Technology

Date: 6 August 2018
Town: Bern

Publisher:
Swiss Federal Office of Energy SFOE
Energieforschung
CH-3003 Bern
www.bfe.admin.ch

Agent:
Empa
Swiss Federal Laboratories of Materials Science and Technology
Überlandstrasse 129, CH-8600 Dübendorf
www.empa.ch

Authors:
Wim J. Malfait, Empa, wim.malfait@empa.ch
Lukas Huber, Empa, lukas.huber@empa.ch
Matthias M. Koebel, Empa, matthias.koebel@empa.ch

SFOE head of domain:
Andreas Eckmanns, Forschungsbereichsleiter, andreas.eckmanns@bfe.admin.ch

SFOE programme manager:
Rolf Moser, BFE-Forschungsprogrammleiter, moser@enercom.ch

SFOE contract number: SI/501462-01

Swiss Federal Office of Energy SFOE
Mühlestrasse 4, CH-3063 Ittigen; postal address: CH-3003 Bern
Phone +41 58 462 56 11 · Fax +41 58 463 25 00 · contact@bfe.admin.ch · www.bfe.admin.ch

Zusammenfassung

Aerogele haben ein beachtliches Potential als Hochleistungsdämmstoff im Gebäudesektor – die Umsetzung am Markt ist allerdings durch teure Prozesses und dadurch bedingte hohe Materialkosten stark eingeschränkt. Dieses BFE Projekt zielt darauf ab, offene wissenschaftliche, technische und verfahrenstechnische Fragen in Bezug auf die Lösemitteltrocknung (LMT) von Aerogelen zu klären und zwar im Vergleich mit der klassischen Methode der überkritischen Trocknung (ÜT). Auf Seite der Grundlagen wurde im Rahmen des Projekts eine Röntgenmikrotomographhiezelle aufgebaut womit die Trocknung in-situ verfolgt werden kann. Zudem wurden neuartige Biopolymere als Modellsystem mit tiefen Wärmeleitfähigkeiten von 23-26 mW/(m·K) für LMT und 16 mW/(m·K) für ÜT entwickelt, wobei diese als monolithische Körper mit hoher spezifischer Oberfläche und Mesoporenanteil die ersten über LMT zugänglichen Biopolymeraerogele dieser Art in der Literatur sind. Sowohl die Tomographieuntersuchungen als auch die Biopolymeraerogele werden als SNF Projekt weitergeführt. Auf Seiten der angewandten Forschung, wurden diverse Parameterfelder untersucht und dabei die Wichtigkeit hoher Temperatur und Schleppgasraten entdeckt. Ebenso zeigte sich, dass eine quantitative Rückgewinnung der Lösemittel eine Herausforderung ist. Eine Reihe bekannter und neuer Trocknungsansätze wurden verfolgt, unter anderem auch Vakuumtrocknung sowie konvektive Gastrocknung mit einer Kaskade von Kondensatoren. Zudem wurde die Wiederverwendung von zurückgewonnenem Lösemittelgemisch in der Gelsynthese experimentell bestätigt. Die aus dem Projekt hervorgegangene Trocknungstechnik wird derzeit in einer durch das BFE P&D Programm unterstützten Pilotanlage umgesetzt. Die Vorteile der Methode im Bezug auf reduzierten Energieverbauch und grauem CO_2 wurde mittels Ökobilanz bestätigt. Das Projekt konnte eine wichtige Hürde in Richtung Massenproduktion von SiO_2 Aerogelen mittels LMT überwinden.

Résumé

Les aerogels offrent un potentiel remarquable comme matériau d'isolation haute performance dans le secteur du bâtiment. Cependant, la réalisation pratique est restreinte par une technologie de fabrication coûteuse et des frais de matériaux élevés qui en résultent directement. Ce projet BFE ciblait à résoudre des questions scientifiques, techniques et d'ingénierie liées au séchage sous pression ambiante (SPA) des matériaux d'aerogel, une téchnologie qui compte à remplacer le séchage supercritique (SSu) plus complexe à l'échelle industrielle. Concernant les aspects scientifiques fondamentaux, une nouvelle étape de chauffage pour étudier la SPA des aerogels de (silice) in situ avec la microtomographie à rayons X a été conçue et construite. De plus, de nouveaux aerogels de biopolymères réticulés ont été développés avec des conductivités thermiques très faibles - 16 mW / (m·K) pour le SSu et 23-26 mW / (m·K) pour le SPA. Notamment, les aerogels SPA sont des échantillons monolithiques intactes présentant une grande surface spécifique et une grande mésoporosité, ce qui les rend uniques dans la littérature des aerogels à base de biopolymères. Les activités tomographie "in-situ" et aerogels biopolymères sont les deux transférés dans un projet de suite supporté par le FNS. Quant aux aspects application, une série d'études de paramètres soulignent l'importance des températures de séchage élevées et des débits de gaz élevés pour un séchage rapide et une production de matériaux d'aerogel de haute qualité et de faible densité. En même temps, ces expériences soulignent les difficultés à atteindre des taux de récupération de solvants suffisamment élevés, particulièrement à l'échelle laboratoire. De divers concepts de séchage existants et nouveaux ont été évalués, y compris un séchage sous vide partiel dans un réacteur conique avec un condenseur intégré et un séchage par évaporation à pression ambiante avec une cascade de condenseurs. Le recyclage du solvant récupéré sans purification intermédiare a été établi grâce à étude de conception expérimentale. Enfin, la solution de séchage sélectionnée est actuellement mise en œuvre dans une installation pilote dans le cadre d'un projet récemment secondé par le programme P&D de l'OFE. L'analyse du cycle de vie du concept de production confirme l'efficacité énergétique et les émissions de CO2e limitées du procédé. Dans l'ensemble, le projet a surmonté une étape importante vers la production industrielle des aerogels de silice par séchage à pression ambiante.

Summary

Aerogels offer a remarkable potential as high-performance insulation material in the building and construction sector – yet the practical realization is impaired by costly process technology and high materials cost which comes as a direct result. This BFE project aimed to solve open scientific, technical and engineering questions related to ambient pressure drying (APD) of aerogel materials, as an alternative to the more complex supercritical drying (SCD) process. On the fundamental, scientific front, a new heating stage to study APD of (silica) aerogels in situ with X-ray microtomography was designed and constructed. In addition, new cross-linked biopolymer aerogels were developed with thermal conductivities as low as 16 mW/(m·K) for SCD and 23-26 mW/(m·K) for APD. Importantly, the APD aerogels are intact, monolithic plates with high surface area and large mesoporosity, making them unique in the biopolymer aerogel literature. Both the in situ tomography and biopolymer aerogels are carried over to a follow-up SNSF project. On the applied front, a range of parameter studies highlight the importance of high drying temperatures and high gas flow rates for fast drying and the production of high quality, low density aerogel materials. At the same time, these experiments point to the difficulties in achieving sufficiently high solvent recovery rates, particularly at laboratory scale. A variety of existing and new drying concepts were evaluated, including a conical drying under partial vacuum with an integrated condenser and evaporative drying at ambient pressure with a cascade of condensers. The recycling of recovered solvent without prior purification was established through an experimental proof-of-concept. Finally, the selected drying solution is currently implemented in a large pilot facility as part of a recently awarded SFOE P&D project. Life cycle assessment of the production process confirms the energy efficiency and limited CO_2e emissions of the chosen production route. All in all, the project has provided an important step towards the mass production of silica aerogels through ambient pressure drying.

Contents

List of abbreviations

APD	Ambient pressure drying
SCD	Supercritical drying
HMDSO	Hexamethyldisiloxane
TEOS	Tetraethoxysilane
MEK	Methyl ethyl ketone
EtOH	Ethanol
LCA	Life cycle analysis
LCC	Life cycle cost

1. Departure point and boundary conditions

1.1 Current state of industrial silica aerogel production

The industrial production of silica aerogel constitutes a global annual market of ca. 300 Mio CHF with rapid annual growth rated on the order of 20% [1]. Market leader Aspen aerogel has a market share of ca. 50% and most of its production consists of silica aerogel blankets that are produced from silicon alkoxide precursors through a supercritical CO_2 drying process. Cabot aerogel is market leader for silica aerogel granulate and produces from a waterglass precursor and ambient pressure drying. Thus, the world's two largest silica aerogel producers utilize different precursors and different drying conditions. There are a variety of other, young companies that enter the market and also here, both types of precursor, and both types of drying methods are utilized. Concerning the relative merits of both drying processes, supercritical CO_2 drying is industrially now well established, but requires complex, high pressure autoclaves and is inherently a batch-type process. Ambient pressure drying relies on simple heating and requires less complicated equipment and is potentially a continuous process, but has not been implemented at the scale of supercritical CO_2 drying for industrial production. In addition, open scientific questions about the behaviour of aerogels during evaporative drying remain.

1.2 The Empa one-pot process

During the last decade, Empa has developed a new silica aerogel production process that minimizes solvent consumption, production time, and ultimately, production cost [2]. This so-called one-pot process introduces the hydrophobization agent into the sol prior to gelation, but activates it only after gelation has been completed. Some of the big open questions that motivated this project were the unknowns about the ambient pressure drying process detailed in 1.1.

1.3 Biopolymer and biopolymer-silica hybrid aerogels

During the last decade, Empa has developed a variety of biopolymer reinforced silica aerogels that combine the excellent insulation properties of silica aerogel with increased mechanical strength, lower dust release, and sustainable precursors [3]. At the start of the project, all these materials required supercritical CO_2 drying for their production, which was identified as one of the major bottlenecks for upscaling.

1.4 Boundary conditions

For the more fundamental scientific part of the project on the fundamental aspects of ambient pressure drying, also of biopolymer based aerogels, the main boundary condition was that scientifically relevant data, collected to the highest quality standards was collected and interpreted correctly. For the more applied part of the project that deals with ambient pressure drying of silica aerogel, only commercially viable and industrially and technically feasible solutions were to be pursued, as the ultimate goal was to move closer towards the mass production of silica aerogels through ambient pressure drying.

2. Project aims

The ultimate goal of this proposal is to provide cost-effective, improved insulation materials for retrofitting buildings with space restrictions. We will achieve this target by paving the way for the large-scale, cost- and energy-effective production of aerogels with improved mechanical properties by removing the barrier of SCFD.

- For silica aerogel, the goal is **an optimized APD drying process with reduced drying energy demand** resulting in a lower overall embedded energy of the material, quantified by Life Cycle Analysis and Life Cylce Cost Analysis (LCA and LCC) methods.
- For (bio)polymer reinforced silica aerogels, the goal is to **develop and establish an APD protocol** to produce materials with **properties comparable to aerogels dried by SCFD**.

3. Sample characterization

The envelope density (ρ) was obtained by a Geopyc 1360 (Micromeritics). A 12.7 mm diameter chamber was used to measure with a consolidation pressure of 4 N. 10 cycles were carried out for each measurement.

SEM was performed for microstructural analysis after coating with 15-20 nm of Platinum. SEM images were recorded with a FEI Nova NanoSEM 230 at an acceleration voltage of 10 kV and a working distance of 5 mm.

N_2 adsorption and desorption isotherms at 77 K were collected (Micromeritics 3Flex) after degassing approximately 100 mg silica aerogel granulate at 250°C for 40 hours at 1.6×10^{-2} mbar. The total surface area and volume fraction of mesopores was calculated from the sorption isotherms by the Brunauer-Emmet-Teller (BET) method [4] and Barrett-Joyner-Halenda (BJH) analysis [5], respectively. It is known, that aerogel samples experience mechanical deformation in the desorption branch of the capillary condensation range [6].

NMR spectra were recorded on a Bruker Avance III spectrometer equipped with a wide-bore 9.4 T magnet, corresponding to Larmor frequencies of 400.2 MHz for ^{1}H, and 79.5 MHz for ^{29}Si.

The thermal conductivity of small samples was determined using a custom built guarded hot plate device (measuring zone of 25 × 25 mm^2) which was designed for small samples of low conductivity materials [7]. One side of the asymmetric configuration was heated to 30°C with the other side cooled to 12°C.

LCA assessment life cycle is a modular system where the main stages are the product and construction stage (A), the use stage (B) and the end of life stage (C). We limit our analysis to the product life cycle, i.e. a cradle to gate approach, as the use and end of life stages are beyond the scope of this study. Thus, the following life cycle sub-stages are taken into account: raw-material acquisition (life cycle stage A1), raw-material transportation (life cycle stage A2) and product production (life cycle stage A3). The impact which considered is carbon footprint and it is calculated according to the IPCC 2007 method. The assessment is based on pilot stage one- and two-pot production processes. Various scenarios are considered with respect to solvent recycling and the type of electricity used during production (with either low or high CO2e emissions).

4. Results and discussion

4.1 Work package 1: Fundamental studies on ambient pressure drying

Task 1.1 In situ observation of APD

The main aim of this task is to perform in situ experiments on the drying of silica aerogels to monitor shrinkage, spring-back and crack formation in situ using X-ray microtomography. We will investigate the effect of temperature, type of solvent and solvent partial pressure. A heating stage (Figures 1-2) has been constructed at the Empa workshop based on designs prepared during 2016 (see Annual report 2016). All components of the heating stage have been machined. Multiple proposals for beam-time at the TomCat beamline of the Swiss Light Source (SLS) at the Paul Scherrer Institute (PSI) have been submitted, but were unfortunately declined because insufficient beam-time was available. As a result, these activities cannot be concluded within the current BFE Gelsec project.

However, the heating stage necessary has been constructed and this line of research will be pursued as part of a recent SNF project granted to Dr. Wim Malfait (200021_179000, Biopolymer aerogels for thermal superinsulation, 01.05.2018-31.04.2022). Synchrotron beam-time will be applied for at multiple synchrotron sources in Europe (SLS, ESRF, DESY) to maximize the probability that these experiments can be carried out in a timely manner.

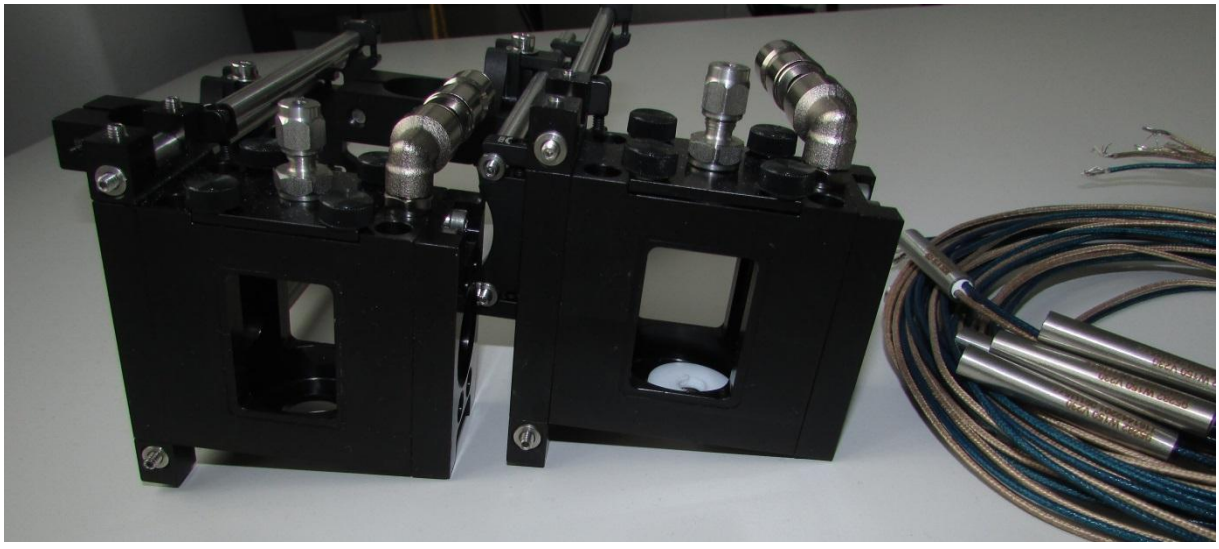

Figure 1. Customized heating stages for in situ X-ray tomography measurements constructed by the Empa workshop and the heating cartridges (right). The stages were constructed in duplicate to maximize the use of the beam-time during the synchrotron experiments.

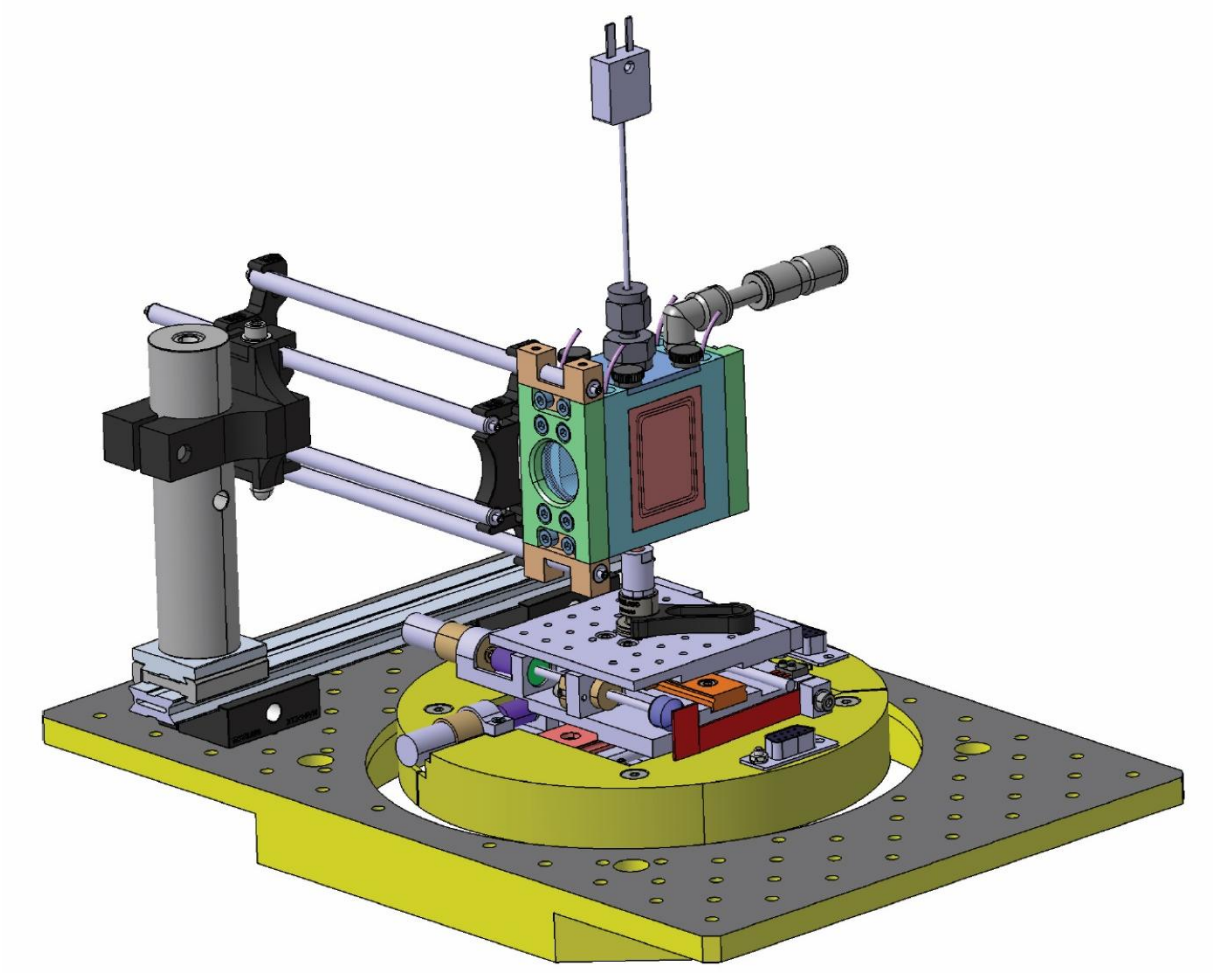

Figure 2. 3D simulation of the heating stage installed at the TomCat beamline at PSI.

Task 1.2 Development of APD for (bio)polymer-silica hybrid aerogels

Whereas APD of silica aerogel is now a well-established (albeit not optimized) process at both the laboratory and industrial scale, APD of (bio)polymer and (biopolymer)-silica hybrid aerogels has not been reported on. During this task, we aim to produce (bio)polymer and hybrid aerogels by ambient pressure drying at the laboratory scale.

Pectin-silica aerogels

The first system we use are pectin-silica aerogels, developed in part during the BFE Waterglass project (SI/500777-01) which display improved mechanical properties, but retain the ultralow thermal conductivity of silica aerogels [3a]. A first set of drying experiments was performed from an n-heptane-hexamethyldisiloxane (HMDSO) mixture, whose low surface tension should be beneficial for APD. The samples were kept at 65°C for 2 hours in a covered sample container, i.e. at high solvent partial pressure, followed by 150°C for another 2 hours with an open container, i.e. at low solvent partial pressure. During drying, the samples cracked into relatively large pieces (Figure 3) and experienced ca. 18% linear shrinkage, resulting in a final density of ~0.15 g/cm^3. The combination of high linear shrinkage with a relatively low density indicates that significant amounts of material were dissolved during the (acidic) hydrophobization steps. The relatively brittle nature of the materials, compared to the samples prepared by supercritical drying (SCD) following a different hydrophobization regime [3a], also seem to bear this out.

Figure 3. Silica-pectin hybrid aerogels prepared by APD from heptane-HMDSO at 65/150°C.

Polymer-silica aerogels

The second system consists of a synthetic polymer reinforced silica aerogel developed at Empa with an industry partner [8]. Just as for the pectin-silica system, the reinforcement did not come at the cost of an increased thermal conductivity when dried from supercritical CO_2 and the production process is relatively simple compared to the pectin-silica aerogels, albeit with non-renewable precursors. Extensive testing was performed along different strategies with the aim of producing materials of similar quality by APD. Gels were dried using different polymer/silica ratios, using mixtures of different polymers, using highly efficient hydrophobization agents (trimethylchlorosilane), from different solvents (heptane, hexamethyldisiloxane, ethanol and mixtures thereof), using different temperatures (80 to 150°C, including multi-step routines) and under different solvent saturation conditions (gas atmosphere close to saturation versus high flushing rates with dilute solvent concentrations). Unfortunately, none of these strategies were successful in avoiding excessive shrinkage during APD and no materials with a density

below 0.3 g/cm^3 were produced (Figure 4). For comparison, low thermal conductivity silica aerogel has a density of 0.1 g/cm^3.

Figure 4. APD of polymer reinforced silica aerogels for three different types of polymers. Polymer-silica aerogels exhibit high shrinkage during APD regardless of polymer type or drying conditions.

Cross-linked polysaccharide aerogels

Within another internal project, we recently discovered a process that enables cross-linking polysaccharide aerogels. Gels produced in this process are much more rigid compared to standard biopolymer aerogels. Although these materials have not been optimized yet for thermal conductivity, the best samples, prepared by supercritical drying, have a thermal conductivity of 23 mW/(m.K), which is higher than that of silica aerogel, 15 mW/(m.K), but lower than that of air (26 mW/(m.K), with a further optimization potential present. Because the gels are very rigid, we hypothesised that they may be able to withstand the forces that occur during APD and this was indeed confirmed by first drying experiments. The first APD aerogels were relatively robust monoliths (no cracking) and display a typical mesoporous aerogel structure and nitrogen sorption curves (Fig. 5), a surface area on the order of 200 m^2/g and a thermal conductivity of 28 mW/(m.K), even though the materials have not been optimized for the latter. The first APD aerogels were relatively robust monoliths (no cracking, Figure 6).

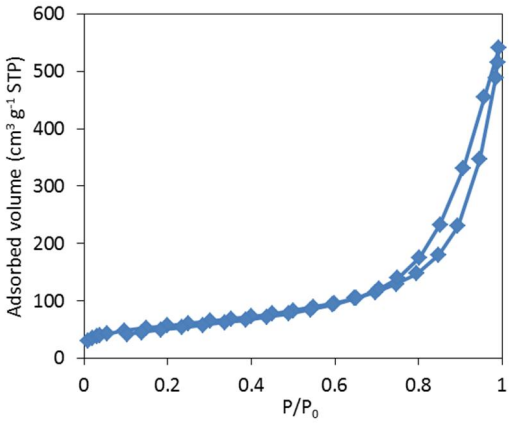

Figure 5. Nitrogen sorption curve of ambient pressure dried cross-linked polysaccharide aerogels.

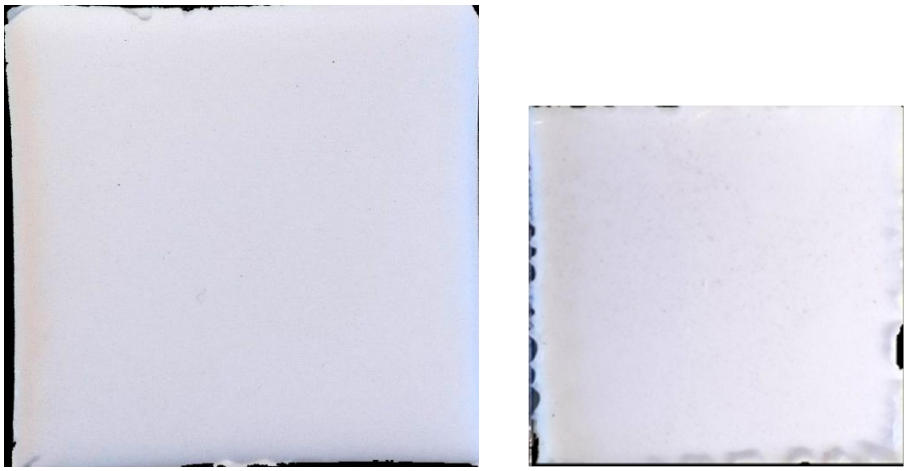

Figure 6. Supercritical (left) and ambient pressure dried (right) biopolymer monolithic aerogels.

During 2017, we have undertaken an extensive program to optimize these materials, both by supercritical and ambient pressure drying. As a result, the thermal conductivity under dry conditions has been reduced from 23 to 16 mW/(m.K) for the supercritical materials (Figure 3). As a result, these materials are now competitive with silica aerogel in terms of thermal conductivity. The materials prepared by ambient pressure drying still display higher densities and the reduction in thermal conductivity has been more limited: from 28 to 26 mW/(m.K). The higher thermal conductivities of the APD materials can be correlated to the partial collapse of the biopolymer skeleton (Figure 7), leading to higher solid conduction through the thicker skeleton, and higher gas phase conduction inside the larger pores.

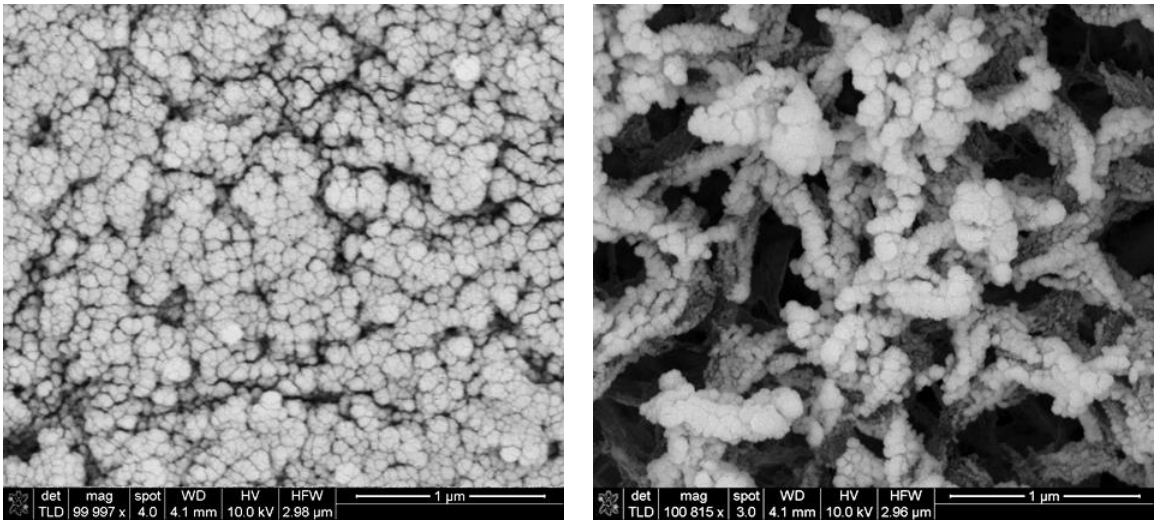

Figure 7. SEM images of cross-linked biopolymer aerogels prepared by supercritical (SCD, left) and ambient pressure drying (APD, right). Note the plate-like morphology due to partial collapse of the solid skeleton during APD.

During 2018, we have continued the extensive research to optimize these materials, both by supercritical and ambient pressure drying. The dataset of thermal conductivity of APD aerogels has been expanded in 2018 (Figure 8). Note that despite progress in the area, the density and thermal conductivity of the APD aerogels (red markers) remains higher than those of their SCD counterparts (blue markers). The APD aerogels still undergo a substantial shrinkage during drying, which raises the density and solid conduction through the biopolymer skeleton. Despite the worse material properties of APD compared to SCD, it is important to note that with a thermal conductivity as low as 26 mW/(m.K), the APD aerogels outperform all conventional insulation materials (glass/mineral wool, EPS, XPS) apart from polyurethane foam. It is also important to note that the APD aerogels prepared in this project are the best APD aerogels presented in the scientific literature.

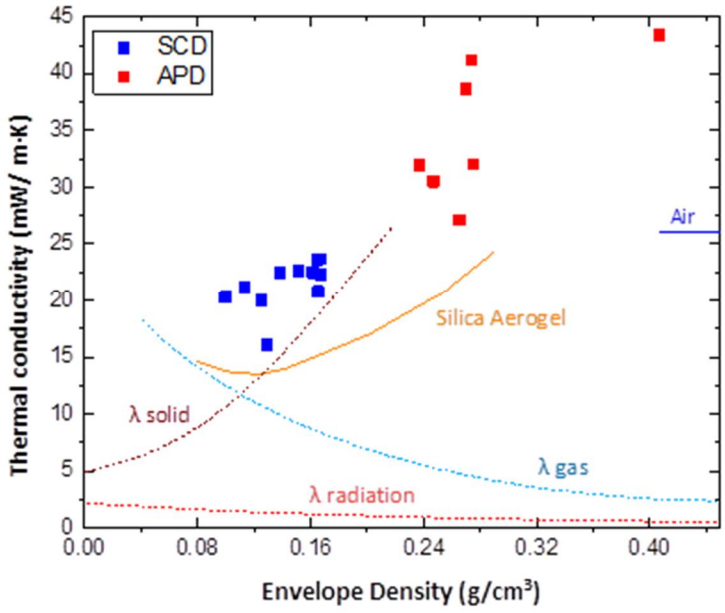

Figure 8. Thermal conductivity versus density of polysaccharide aerogels developed in this project.

Both the SCD and APD aerogels have been characterized by nitrogen sorption analysis to determine the surface area and mesoporosity (both properties are critical for reducing thermal conductivity). Regardless of the initial chitosan concentration, all APD aerogels display type IV isotherms typical of mesoporous materials and aerogels (Figure 9). The best APD aerogels have surface areas around 150 m^2/g, which is comparable to the lower end in surface area obtained by SCD (Figure 9). However, all APD aerogels display higher densities.

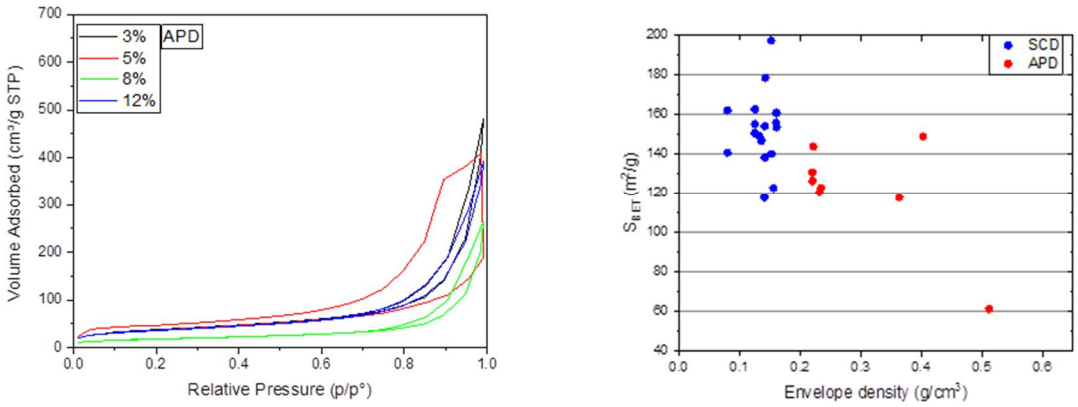

Figure 9. (left) Nitrogen sorption isotherms of biopolymer aerogels prepared by APD. (right) Surface area versus density for both SCD (blue markers) and APD (red markers) aerogels.

One key observation is that the thermal conductivity of the aerogels strongly depends on humidity, with an increase between 5 and 10 mW/M.K) even for the modest increase in relative humidity from basically zero to 30% (Figure 10). This humidity dependence is present for both the supercritically dried (SCD) and ambient pressure dried (APD) aerogels. The strong humidity dependence of thermal conductivity is related to the abundant hydrophilic groups (hydroxyls, urea) on the biopolymer aerogels. These hydrophilic groups most likely are also one of the main reasons for the excessive permanent densification during APD. Thus, hydrophobization will be a key production step to reduce the APD thermal conductivities towards the values obtained for silica aerogel.

During 2018, we undertook an optimization of the APD process, most notably the drying solvent and drying temperature. It was observed that increasing the drying temperature from 25 to 65°C lead to a 15% decrease in thermal conductivity (Figure 11).

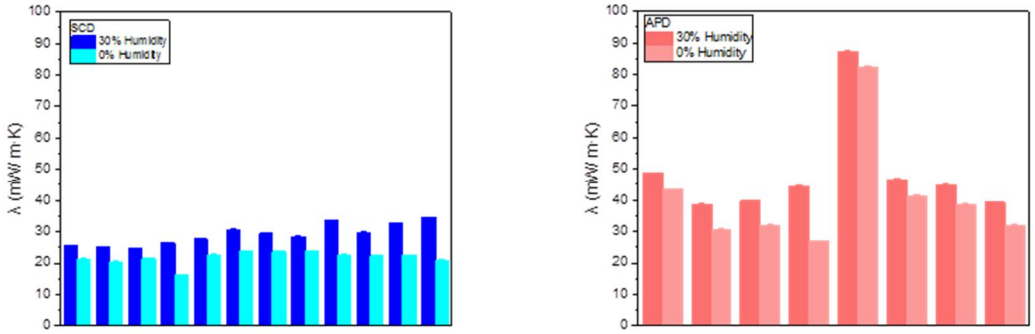

Figure 10. Dependence of thermal conductivity on relative humidity for cross-linked polysaccharide aerogels for supercritical drying (left, blue) and ambient pressure drying (right, red).

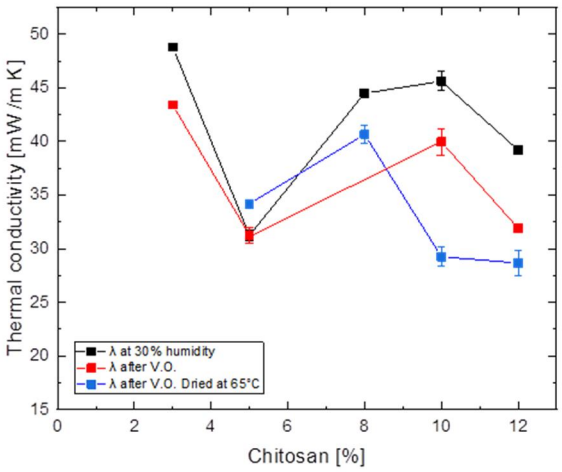

Figure 11. Effect of drying temperature on APD aerogel thermal conductivity.

Summary Task 1.1.2

In summary, our extensive APD experiments for the polymer reinforced silica hybrid aerogels and our preliminary experiments for the pectin-silica hybrid aerogels until now have been mostly unsuccessful, despite the numerous experimental strategies that were pursued for the former. In sharp contrast to this are the cross-linked polysaccharide aerogels, where the very first attempts succeeded in APD of aerogels with material properties that, although not as good as silica aerogel yet, hold great promise. These materials have been further optimized, leading to the following conclusions: a change in the ambient pressure drying protocol to higher temperatures has led to a decrease in thermal conductivity of up to 15%, although the best performing thermal conductivities are still significantly higher than the best-performing SCD samples. Hydrophobization was identified as a key requirement for ambient pressure drying of these biopolymer silica aerogels. The activities will be continued as part of the new SNF project (200021_179000).

4.2 Work package 2: Optimization and upscaling of APD processes

Task 2.1 Evaluation of different drying concepts

Drying under partial vacuum: conical dryer with integrated condenser

In order to evaluate the usefulness of conical drying under partial vacuum, we rented a pilot-scale conical dryer with integrated condenser for 2 weeks of experimentation (Figure 12). The dryer consists of a conical vessel that is heated up through the walls of the cone. A screw is mixing the material to improve heat transport to the gel and improve the homogeneity of the temperature. This equipment was tested under various temperature/pressure regimes, using pilot-produced silica gel granulate as starting material. The aerogel granulate was prepared at the pilot scale using the one-pot process [2b].

Figure 12. Conical dryer with the cooling unit.

At the top of the conical dryer was a glass window, where the drying process can be visually inspected. It was observed that longer drying times lead to a higher fraction of aerogel powder. This was confirmed by the samples which were taken during drying after each hour. After six hours of drying, the aerogel granulates became smaller and the fraction of powder increased significantly (Figure 13-14). In addition, longer drying times result in denser aerogel granulate.

Figure 13. One-pot granulate after drying for one hour in the conical dryer

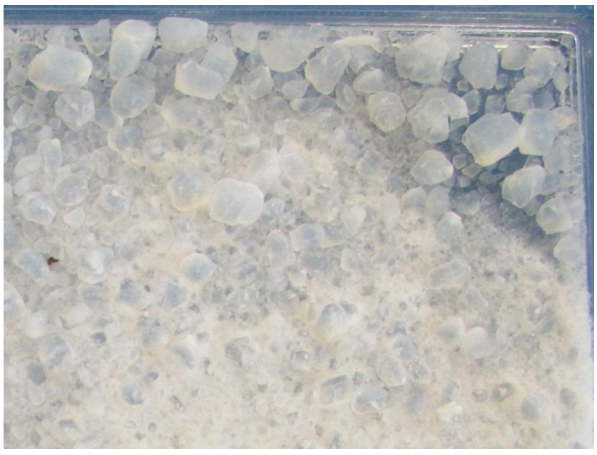

Figure 14. One-pot granulate after drying for six hours in the conical dryer

Although these experiments did not produce silica aerogel granulate of sufficient quality, they did provide information on the various aspects of the APD process. Mixing the granulate during drying results in the generation of powder, rather than granulate, and this is not a suitable process for silica aerogel production. In addition, the experiments highlight the importance of an efficient heat transport through the gel granulate bed.

BFE - Conical Dryer - Batch 25

Sample Code	Drying time (h)	Density (g/cm^3)				
		Run 1	Run 2	Run 3	Average	Standard Deviation
BATCH25/1	1	0.186	0.263	0.179	0.209	0.046
BATCH25/4	4	0.245	0.265	0.243	0.251	0.012

Systematic parameter studies of APD of silica aerogel granulate and silica aerogel composites

The speed of drying is a critical parameter to avoid excessive shrinkage during APD. We therefore conducted a series of systematic drying experiments, where we monitored the weight loss of aerogel granulate beds and aerogel composites as a function of temperature, time and composite thickness. The gel granulate was prepared at the pilot scale using the one-pot process [2b]. The alcogel granulate was dried in ~750 g batches using a 30 cm x 30 cm x 3 cm aluminum frame with a glass fiber mesh bottom (Figure 15). The composite was of similar size. The temperature of the oven was set to the drying temperature. Then, the frames with the composite and the granulate (~750 g) were placed in the middle of the oven. Every 10 minutes, the frames were removed from the oven in order to record the mass. During the drying experiments the oven was opened and closed every 10 minutes in order to determine the weight. This procedure had a negative influence on the temperature stability of the oven. For example, when the temperature set point (T_s) was 150°C, the actual temperature (T_a) before opening was 140°C and after opening the temperature was only 100°C. These interruptions in the drying process may have a negative effect on the quality and the density of the dried aerogel, but the observed trends are nevertheless significant.

Figure 15: Granulate after drying for 40 minutes at 150°C.

It was observed, that the granulate samples dried inhomogeneously. Close to the frame (outer side), the granulate dried faster than in the middle of the frame (Figure 15). This might be attributed to the better heat conduction from the aluminum to the granulate, which increases the drying speed.

Figure shows the influence of the temperature on the relative weight of the aerogel granulates during drying. It can be observed, that higher drying temperatures lead to a faster decrease of the relative weight, i.e. a faster evaporation of the solvent. When the drying temperature is 140°C or higher, the granulate is dry after 2 hours. However, without interruption of the drying process (to weigh the samples), the aerogel granulate would have been dry already after 90 minutes. The hydrophobic aerogel composite with 2 cm thickness, i.e. the same as for the granulate bed, displays similar weight loss curves compared to the granulate bed (Figure 17a), but thicker composites (4 cm) require longer drying times (Figure 10b). This thickness dependence confirms the result from the vacuum drying experiments which highlighted the importance of heat transport into the gel.

Further experiments on hydrophilic aerogel composites indicated that longer drying times are required for hydrophilic materials (not shown), possibly due to the fact that it requires more energy to remove molecules from a hydrophilic surface than from a hydrophobic surface.

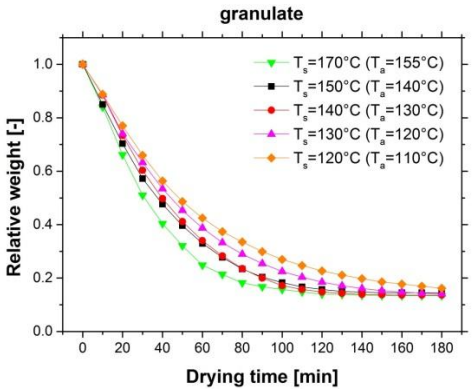

Figure 16: Weight loss of the one-pot granulate during drying at different temperatures.

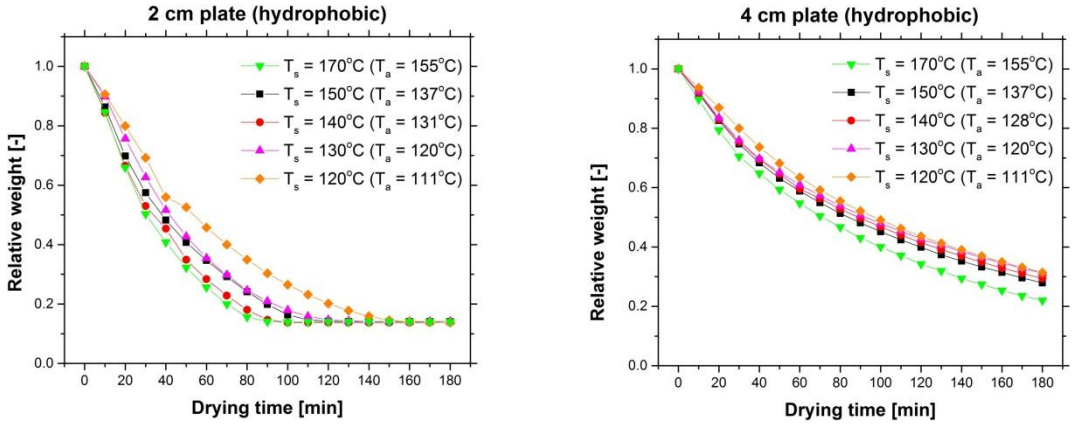

Figure 17: Evolution of the relative weight of the 2 (left) and 4 cm (right) thick aerogel composites.

A second set of drying experiments was performed on the aerogel granulate, where the drying protocol includes a pre-drying at 85°C for 30, 60 or 90 minutes, followed by drying at 150°C. This mimics typical drying protocols form the scientific literature and could, theoretically result in less fragmented materials (i.e. larger granules). Figure 18 shows the evolution of the relative weight after pre-drying the aerogel granulate at 85°C for 30 minutes, 60 minutes and 90 minutes. After 30 minutes of pre-drying the weight loss was 24 wt.%, after 60 minutes 41 wt.% and after 90 minutes 58 wt.%. It was observed, that pre-drying for more than 30 minutes increases the density of the dried aerogel. In addition, the grain sizes did not increase, contrary to what was aimed for in this set of experiments.

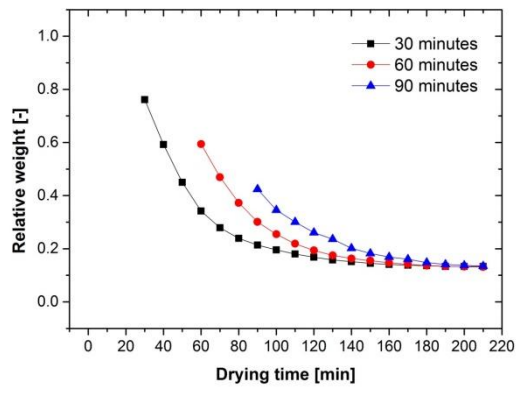

Figure 18: Evolution of the relative weight loss at 150°C after different durations of pre-drying at 85°C.

The envelope density of the various materials was determined by powder pycnometry (Tables 1-3). The target density for superinsulating silica aerogel

is 0.100-0.150 g/cm^3. As discussed above, opening the oven to measure the sample weight has influenced the experiment: samples that were dried without these steps (Table 3) exhibit lower densities than those that did (Table 1). In addition, higher drying temperatures, i.e. faster drying, resulted in lower densities (Table 3). Pre-drying at 85°C negatively affected the sample density, particularly for pre-drying times in excess of 30 minutes (Table 2).

Table 1. Density of the granulate after the drying experiments.

Envelope Density Measurement on Glass fiber mesh

setpoint temperature [°C]	Envelope density based on granules transparency [g/cm^3]		
	Random Granules	Transparent	Non-transparent
120	0.152 ± 0.001	0.165 ± 0.002	0.209 ± 0.005
130	0.148 ± 0.002	0.136 ± 0.002	0.170 ± 0.002
140	0.171 ± 0.003	0.135 ± 0.001	0.168 ± 0.0256
150	0.160 ± 0.004	0.159 ± 0.001	0.184 ± 0.003
170	0.151 ± 0.001	0.132 ± 0.001	0.158 ± 0.002

Table 2. Density of the granulate dried at 150°C after varying times of pre-drying at 80°C.

Pre-drying at 80C, then drying at 150°C

Sample Code	Pre-drying time [min]	Density [g/cm^3]				
		Run 1	Run 2	Run 3	Average	Standard deviation
BFE-30@80-150	30	0.146	0.155	0.136	0.146	0.009
BFE-60@80-150	60	0.184	0.165	0.154	0.168	0.015
BFE-90@80-150	90	0.176	0.163	0.157	0.165	0.010

Table 2 (continued). Density of the granulate dried at 150°C after varying times of pre-drying at 80°C zooming in on short pre-drying times.

BFE - Pre-drying @80 – 150°C - 1Run

Sample Code	Pre-drying time (min)	Density (g/cm3)				
		Run 1	Run 2	Run 3	Average	Standard Deviation
BFE-0@80-150-SO	0	0.115	0.107	0.121	0.114	0.007
BFE-5@80-150-SO	5	0.104	0.113	0.109	0.108	0.004
BFE-10@80-150-SO	10	0.123	0.118	0.117	0.119	0.003
BFE-15@80-150-SO	15	0.113	0.109	0.109	0.110	0.002
BFE-20@80-150-SO	20	0.112	0.106	0.113	0.111	0.004
BFE-25@80-150-SO	25	0.119	0.116	0.116	0.117	0.002
BFE-30@80-150-SO	30	0.122	0.127	0.128	0.126	0.004
BFE-150-SO-REF	Reference	0.120	0.113	0.118	0.117	0.004

Table 3. Density of granulate dried in 1 run without taking out of the oven.

BFE – Single run

Sample Code	Setpoint temperature [°C]	Density [g/cm^3]				
		Run 1	Run 2	Run 3	Average	Standard deviation
BFE-130-1R	130	0.139	0.137	0.132	0.136	0.004
BFE-140-1R	140	0.129	0.127	0.138	0.131	0.006
BFE-150-1R	150	0.119	0.134	0.123	0.125	0.008

Collaboration with industrial drying expert (name is confidential)

Contacts were made with a German based company that specializes in industrial drying processes and the design of drying tunnels. We shipped them alcogel granulate that was prepared at the pilot scale using the one-pot process [2b]. They performed several drying experiments using a high exchange rate of the drying atmosphere (120x/hour, i.e. every minute the gas inside their oven got replaced two times). Compared to our standard drying procedure (which uses a 12 times lower exchange rate), the aerogel granulate was more transparent, but the particle size was smaller. The envelope density of the granulate was measured at Empa (Table 1) and was 0.10 to 0.11 g/cm^3, which is exactly on target. During the drying experiments some small pieces of granulate fell out of the frame and gathered on the bottom plate of the oven. This deposit shows some blue impurities. Furthermore, the graunlate from the deposit are smaller compared to the normal granualtes

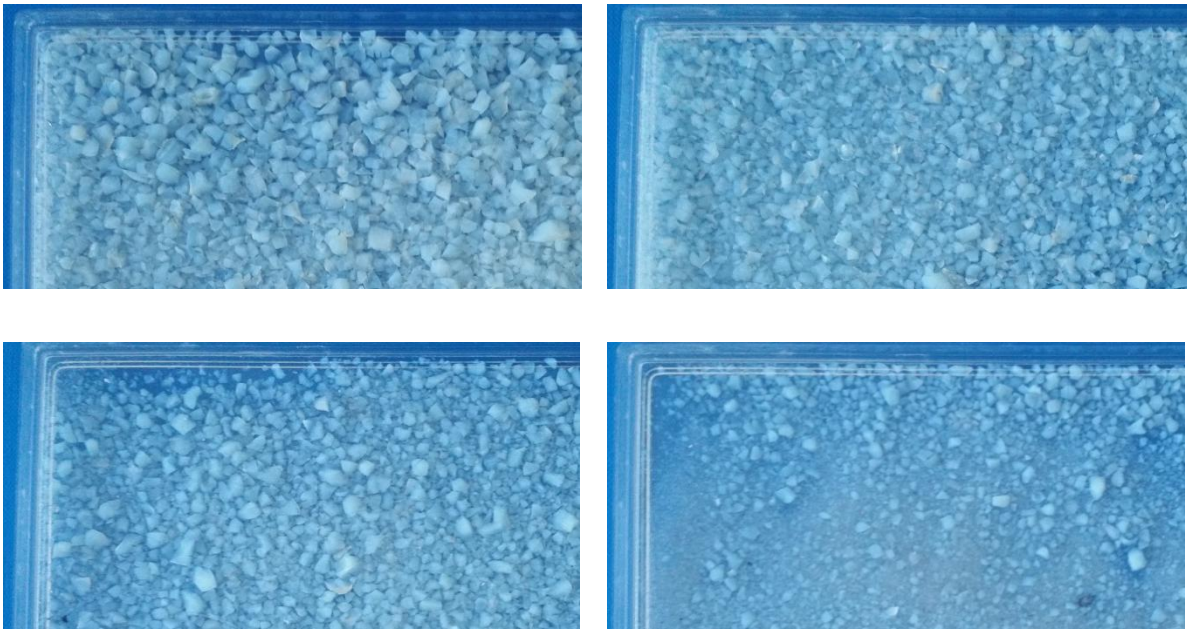

Figure 19. Aerogel granulate dried at high gas exchange rates by the industry partner: Left: test 1, right: test 2, top: granulate, bottom: deposits.

Table 4. Envelope density of the dried aerogel granulate

Sample	Envelope density [g/cm^3]
Batch 33 – standard drying	0.104
Industry-Partner Test 1	0.109
Industry-Partner Test 2	0.100
Deposit of Test 1	0.115
Deposit of Test 2	0.086

Influence of gas exchange rates: systematic parameter studies

During these experiments, ca. 700 g of organogel was placed inside an oven and dried using the temperatures and gas low rates specified in Table 5. The gas coming from the oven was passed through two condensers and its amount and composition determined. Please refer to Task 2.2 for more details on solvent compositions. The aerogel density was found to depend strongly on the gas flow rate, and low density aerogel could only be synthesized at nitrogen flow rates in excess of 5 L/min (Figure 20). Combined with the requirement of sufficiently high temperatures (Annual report 2016), this confirms the notion that efficient, fast drying is required to minimize shrinkage during drying.

Table 5

Sample	Wet gel [g]	Flow rate [L/min]	Bottle1 [g]	Bottle2 [g]	Aerogel [g]	Density [g/cm^3]
Gelsec1	628	2 @ RT	429.3	202.4	85.6	-
Gelsec2	662.2	2 @ 160°C	463.7	213.9	87.7	-
Gelsec3	765	2 @ 160°C	545.9	196.8	101.8	0.197
Gelsec4	716	5 @ 180°C	475.7	224.4	93.8	0.145
Gelsec5	738.5	10 @ 180°C	354.5	267.2	95.6	0.117
Gelsec6	738.2	20 @ 180°C	214.3	254.2	95.9	0.117

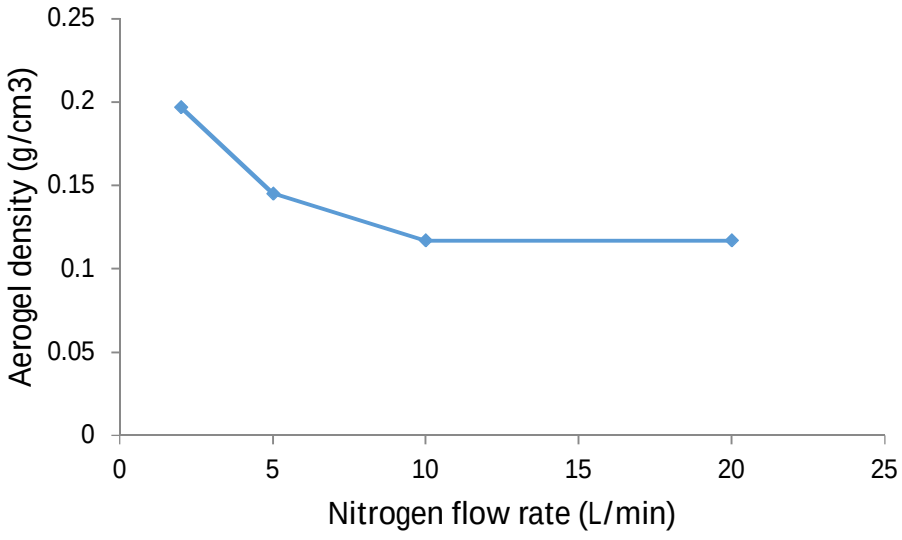

Figure 20. Aerogel density versus carrier gas flow rate.

Solvent recovery: difficulty in achieving a gas-tight system.

Before the experiments on the drying of aerogel, as described above, had been carried out, control experiments have been conducted to verify the efficiency of the solvent recovery. During these experiments, a bottle with ethanol was placed inside the oven and left to evaporate, and the weight of the ethanol in the condenser recorded after the experiment. The results indicated that at most 80-90% of the solvent could be recovered for our experimental setup, and the recovery rate was independent of the condenser temperature (water-ice, water-salt-ice, ethanol-dry ice (CO_2). Theoretical calculations indicate that a recovery of >99% should be possible, particularly for the lowest condenser temperature (Table 6). Because of the independence on condenser temperature during the experiments, we hypothesized that we were losing some of the nitrogen carrier gas and solvent vapour, i.e. not all of the solvent vapour was passing through the condenser. A subsequent smoke test with our oven indeed confirmed that the oven was not gas tight under our conditions. Note that the oven used is a vacuum oven that can effectively hold a vacuum over multiple hours and even days. During our operation at atmospheric pressure however, the oven is not gas tight, i.e. the oven requires a partial vacuum to "self-seal". Additional efforts at improving the seal quality were not successful. Further consulting with engineers in industry and at Empa confirmed that gas tight sealing of conventional drying systems is only possible at significant cost for industrial installation.

Table 6. Theoretical solvent losses as a function of gas flow rate and condenser temperature.

Ethanol vapor pressure

T (°C)	P (mm Hg)	P (kPa)
-15	3.63	0.48
-10	5.44	0.73
-5	8.01	1.07
0	11.59	1.55
5	16.50	2.20
10	23.13	3.08

Loss of ethanol (kg) for a given exchange rate (oven capacity = 60 L), assuming drying takes 1 hour
How much ethanol can pass through the condensor because it is below the vapor pressure at a given condensor temperature
Assuming we are drying off 1 kg of ethanol during the experiment

N2 flow rate (L/min)	2	4	6	8	10	20	40	60
exange rate (oven vol/h)	2	4	6	8	10	20	40	60
condenser T (°C)								
-15	0.1%	0.2%	0.3%	0.5%	0.6%	1.1%	2.3%	3.4%
-10	0.2%	0.3%	0.5%	0.7%	0.8%	1.7%	3.4%	5.1%
-5	0.2%	0.5%	0.7%	1.0%	1.2%	2.5%	5.0%	7.5%
0	0.4%	0.7%	1.1%	1.4%	1.8%	3.6%	7.2%	10.8%
5	0.5%	1.0%	1.5%	2.1%	2.6%	5.1%	10.3%	15.4%
10	0.7%	1.4%	2.2%	2.9%	3.6%	7.2%	14.4%	21.6%

Solvent recovery: loss of solvent from condenser at high flow rates

Our parameter studies above confirmed the need for high gas flow rates to minimize drying related shrinkage and optimize the aerogel quality. The higher flow rate however increases the demand on condenser capacity and design, and this was also clear from our experimental data. For a given condenser system, ethanol is lost from the condenser and carried out with the carrier nitrogen gas at high flow rates (Table 7, Figure 21).

Table 7. Loss of solvent from second condenser bottle (Experiments 6.1 and 6.1).

Flow rate of nitrogen [L/min]	Loss of Ethanol per hour in bottle 2 [g]
2	5.0
10	15.8
20	28.5

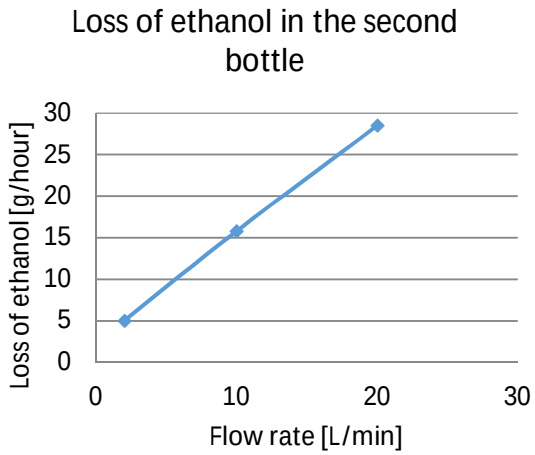

Figure 21. Loss of ethanol from condenser at high flow rates.

Summary Task 2.1

During 2016, we have evaluated various drying concepts and established the importance of drying temperature on final product quality, both for aerogel granulates and fiber meshes (Annual Report 2016). Some of the 2016 results also hinted at the importance of the gas exchange rate for successful drying, and this was pursued systematically during 2017. These experiments confirmed the need for high gas flow rates to achieve minimal shrinkage and good aerogel properties. At the same time, a high gas flow rate presents problems with respect to the leak-tightness of the system and place more stringent constraints on the condenser design. High gas flow rates thus require smart engineering and/or additional capital expenses to minimize solvent losses. In summary, the laboratory experiments confirmed the need for high gas flow rates during drying and hint at the difficulties that are to be expected during pilot implementation of a drying process with high flow rates, with respect to leak tightness and condenser design.

Task 2.2 Development of solvent and waste heat recovery strategy

Silica aerogel from recycled solvent without purification

The LCA analysis (WP3) identified the re-use of recovered solvent without purification as an important step to limit energy consumption during production. We have tested this experimentally in the following way. The solvent recovered after hydrophobization of a pilot scale experiment was analyzed by quantitative ^{1}H NMR (Figure 22) and Karl Fischer titration and consisted of 13 wt% HMDSO, 84 wt% ethanol, 3 wt% water, 1.3 wt% MEK (from the denaturized ethanol starting material) and 0.05 wt% NH_4^+. Note that for this particular batch, the acid catalyst was added with ethanol rather than HMDSO, resulting in a lower HMDSO content of the solvent after hydrophobization.

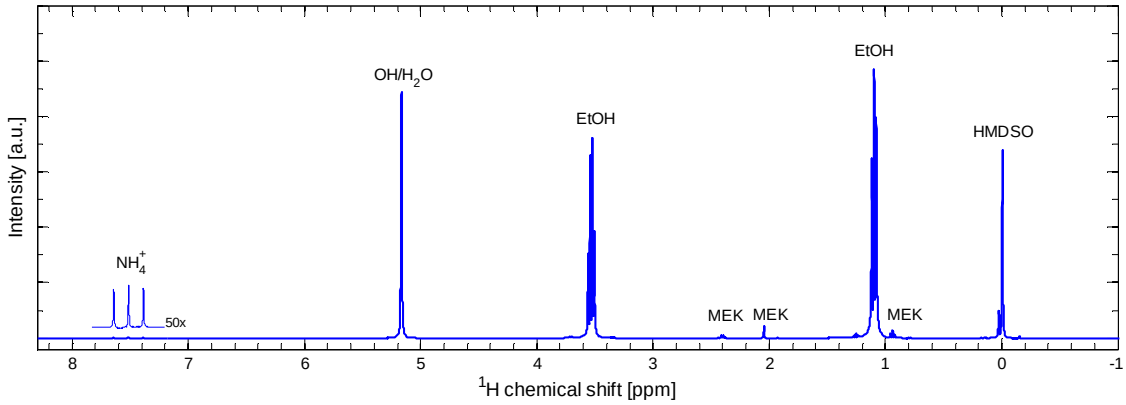

Figure 22. ^{1}H NMR spectrum of the solvent recovered after hydrophobization.

The recovered solvent was then mixed, without purification, with the appropriate amounts of PEDS (P750), virgin HMDSO and ammonia to produce a new batch of silica aerogel using the one-pot process on the laboratory scale. The resulting aerogel, which used 65% of recycled solvent without purification) has a similar density (0.136±0.009 g/cm^3) compared to those prepared exclusively from virgin reagents. This provides proof-of-concept that recovered solvents can be re-used without solvent purification. Note that because the recovered solvent contains a mixture of HMDSO and ethanol, such re-use without purification is only possible using the one-pot process. Recycling without purification potentially leads to the build-up of salts (from the basic gelation and acidic hydrophobization catalysts). In figure 23, we have modelled the evolution of the salt concentration as a function of the number of times the solvent is re-used, for different fractions of solvent recycled without purification. For all investigated re-use fractions, the salt concentrations reach a steady state at a level that are compatible with the sol-gel process.

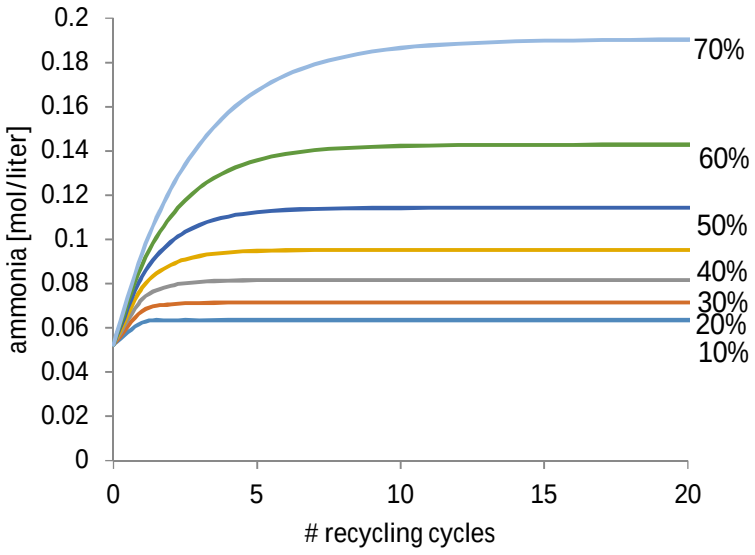

Figure 23. Salt build-up during solvent re-use without purification, for different fractions of re-use (%).

Analysis of recovered solvents

The solvents from the condenser bottles are all acidic (Table 8), as is to be expected based on the acid conditions during the hydrophobization step prior to drying.

Table 8. pH of solutions.

Solution	pH value
Gelsec 1 B1	1.26
Gelsec 1 B2	1.22
Gelsec 2 B1	1.47
Gelsec 2 B2	1.5
Gelsec 3 B1	3.9
Gelsec 3 B2	4.8
Gelsec 4 B1	2.13
Gelsec 4 B2	1.15
Gelsec 5 B1	1.2
Gelsec 5 B2	1.5
Gelsec 6 B1	0.93
Gelsec 6 B2	1.5
used modification solution Batch 44	0.75
syneresis solution Batch 44	7.97
Ethanol with 2% MEK	6.35

The solvent composition was determined by quantitative ^{1}H NMR (Figure 24, Table 9). The various solvent components (ethanol and HMDSO) are well resolved in the spectra (Figure 24) and the intensity ration of the CH_2 to CH_3 bands of ethanol are 1.98:3.00, i.e. identical to the theoretical 2:3 within analytical uncertainty (Table 9). The most striking result from these measurements is the observation that HMDSO is condensed preferentially in the second condenser bottle, often to a very large extent (>90%). This result is highly surprising: because of the higher boiling point and lower vapor pressure (Figure 25) of HMDSO, we expected preferential condensation inside the first condenser bottle. Further research is required to fully understand and characterize this behavior, but this observation is very promising, as it demonstrates that it is possible to do a first separation of the solvents after drying through a well-engineered condenser design. We have previously demonstrated that ~70% of the solvent can be recycled without purification (Annual report 2016). The current observation indicates that the first condensation after drying may be sufficient to separate the remaining 30%. In other words, no additional distillation and solvent work-up may be required.

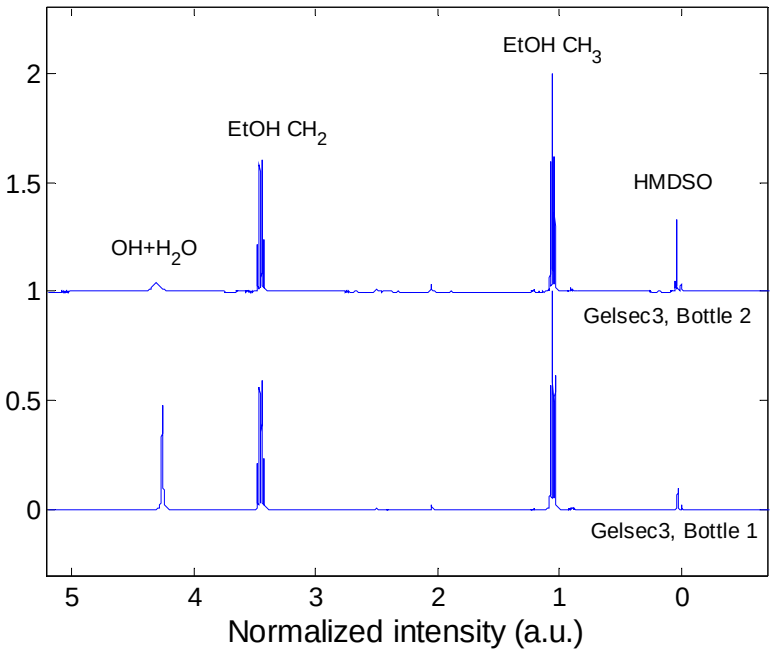

Figure 24. Selected ^{1}H NMR spectra of solutions from the condenser. Note the higher peak for HMDSO in the spectrum of the solution from bottle 2 (top line).

Table 9. Condensate compositions from solution NMR data

		Relative ^{1}H NMR intensities				Solvent composition (mol%)		
Gelsec	Bottle	OH/H2O	EtOH CH2	EtOH CH3	HMDSO	Ethanol	HMDSO	H2O
3	1	1.27	1.97	3	0.16	94.09%	1.67%	4.23%
3	2	1.02	0.197	3	0.45	79.13%	19.56%	1.30%
4	1	1.29	1.98	3	0.06	94.79%	0.63%	4.58%
4	2	1.07	1.97	3	0.32	86.41%	10.23%	3.36%
5	1	1.3	1.99	3	0.01	95.14%	0.11%	4.76%
5	2	1.13	1.98	3	0.04	94.05%	1.01%	4.94%
6	1	1.34	1.99	3	0.02	94.44%	0.21%	5.35%
6	2	1.14	1.99	3	0.03	93.48%	0.81%	5.70%

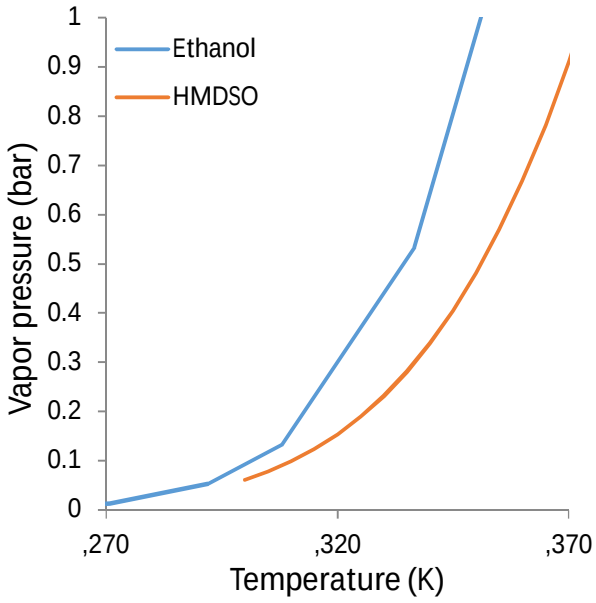

Figure 25. Vapour pressure of ethanol (blue) and HMDSO (orange).

New aerogel production and drying concept and effect on solvent and heat recovery

The work described in Task 2.1, and the various drying and condensation concepts tested highlight the difficulties in designing a system that recovers >98% of the solvents with the current oven test-drying concept. Yet, significant losses of solvent during production are not acceptable from environmental (VOC emissions, overconsumption of raw materials) and commercial (VOC taxes, cost of raw materials) points of view. Thus, the experiences during Task 2.1 have provided valuable information about the limitations of a simple lab-oven prototype system. Motivated in part by these unsatisfactory observations, we have designed and implemented a new aerogel drying concept at small scale (1l) for testing and validation purposes. The basic chemical process and material qualities remain the same: the production is still based on the patented, minimal solvent, Empa one-pot process[2, 9] and the materials have thermal conductivities (~18 mW/(m·K) for granulate bed) and densities (0.110 g/cm^3) typical of high quality silica aerogel. The new drying concept reactor was designed from ground up to be gas-tight. Furthermore, because of the higher volume loading of wet gel (wet gel loading in the new system > 20%$_V$ versus ~1.5-2%$_V$ in the convective drying oven system) both solvent and heat recovery is greatly facilitated through the corresponding reduction of carrier gas volume flow.

The details on the engineering of this new dryer concept are confidential at the moment. Please contact Dr. Wim Malfait or Dr. Matthias Koebel from Empa for more information.

Task 2.3 Construction and commissioning of the drying and recovery installations

Following the parameter studies (temperature, gas flow rate, solvent compositions) and realization of the difficulties in achieving gas tight drying systems with >95% solvent recovery (see annual reports 2016, 2017), a new drying concept which eliminates many of these problems was developed and implemented at the small pilot scale (see task 2.3). The details on the engineering of this new dryer concept are confidential at the moment. Please contact Dr. Wim Malfait or Dr. Matthias Koebel from Empa for more information.

Task 2.4 Pilot production and characterization of APD production process: pure silica aerogel

A larger drying system pilot installation (>50 L batch size) is currently in the commissioning phase, based on the results of the 1l pilot installation described in section 2.3 of the 2017 Annual report. Please contact Dr. Wim Malfait or Dr. Matthias Koebel from Empa for more information. The activities on the pilot production of silica aerogel, including APD, are continued in the recently granted BFE P&D project (SI/501607-01, Pilot scale optimization for cost- and energy-effective silica aerogel production using a disruptive chemical process, 16.09.2017-15.09.2019).

4.3 Work package 3: LCA of different drying concepts

Task 3.1 Life Cycle Analysis

Background

LCA assessment life cycle is a modular system where the main stages are the product and construction stage (A), the use stage (B) and the end of life stage (C). We limit our analysis to the product life cycle, i.e. a cradle to gate approach, as the use and end of life stages are beyond the scope of this study. Thus, the following life cycle sub-stages are taken into account: raw-material acquisition (life cycle stage A1), raw-material transportation (life cycle stage A2) and product production (life cycle stage A3). The impact which considered is carbon footprint and it is calculated according to the IPCC 2007 method. The assessment is based on pilot stage one- and two-pot production processes. Various scenarios are considered with respect to solvent recycling and the type of electricity used during production (with either low or high CO_2e emissions).

Preliminary considerations

The data and technology under evaluation is based on the pilot stage 'one and two pot production' process as described in the methods section of the main text. In chemical industry most processes produce more than the intended substance and the material flows are not usually distributed in a simple way. During aerogel production, many chemicals are used but only a fraction of those are retained in the end product. It is crucial for the results, how the used chemicals are considered within the manufacturing process and this assessment is based on pilot scale testing results (as no operating production plant is operational at this time). Thus, the recyclability of the removed solution is a theoretical approach based on the experience at the pilot scale. The possibilities are to consider 1) that all used substances have a virgin origin, or 2) that part of the removed (produced) solutions are available for re-using them in the next aerogel batch process or otherwise else. In this assessment, two options were considered:

1. 'no recycling' case: all substances are virgin and those which not retain into the product considered as a waste.
2. 'recycling' case: ethanol and HDMSO are recycled within a close loop system (Figure 26) with a recycling efficiency of 98% and 2% of losses. The recycling process resulting to the process when more ethanol is generated than is used. We assume that 70% of the recovered solvent (a mixture of ethanol, HMDSO, water and salts) can be recycled without purification, whereas 30% undergoes purification to allow for the removal of excess ethanol, water, and salts. The purification step consists of the phase separation and decantation of HMDSO through the addition of water. The remaining ethanol-water-salt mixture is then purified through distillation [10]. The aerogel production process results in two product outputs: aerogel and excess ethanol derived from the hydrolysis of TEOS. In this evaluation, we consider that the excess ethanol is sent back to the TEOS producer after purification. The process producing also ammonium chloride and ammonium sulphate in minor amounts. Their reuse is not known and not considered and these products are considered waste and their use amounts are allocated to the aerogel production.

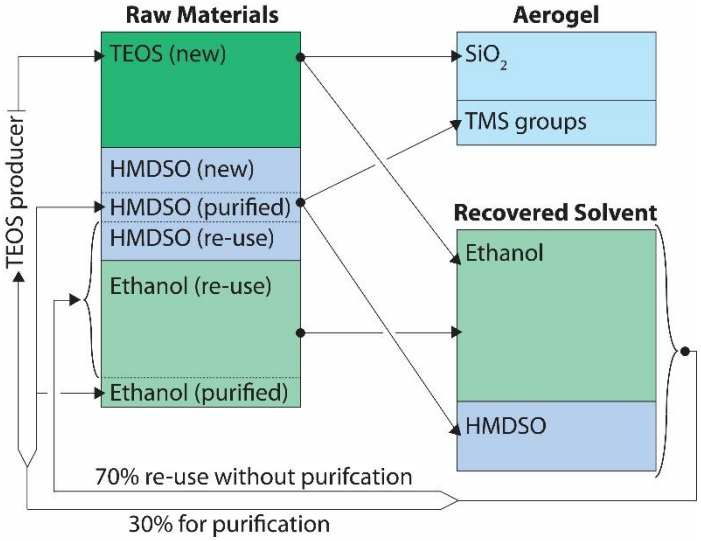

Figure 26. Solvent recycling as considered during the LCA analysis ('recycling' case) for the one-pot process. For the two-pot process, all of the recovered solvent requires purification prior to re-use as the sol is free of HMDSO.

CO_2e for aerogel raw-materials (A1)

Main substances causing carbon footprint within used raw-materials in aerogel production are TEOS, HMDSO and ethanol. With solvent recycling, the aerogel production produces more ethanol than needed for the process: no virgin ethanol is needed and the excess ethanol is recycled back to the TEOS producer. The CO_2e allocated to ethanol is related to the purification, where the energy for purification is based on Ref [10]. The main raw-materials which needed for aerogel production are:

- Ethanol. Within this assessment the ethanol production and LCA data based on the literature [11] for ethanol produced from sugar beet in France. This assessment considers the process when ethanol is made in co-production which the pulp. The impact allocation between these main products (ethanol and pulp) is made. The basis of allocation was economical with an allocation factor for the ethanol of 89%.

- Hexamethyldisiloxane. HMDSO is an organosilicon compound with the formula $O[Si(CH_3)_3]_2$. Hexamethyldisiloxane is produced by hydrolysis of trimethylsilyl chloride ($(CH_3)_3SiCl$). LCA data for hexamethyldisiloxane was not found and the data in this calculation are based on the hexamethyldisilazane from EcoInvent database [12]. Both chemicals are made from trimethylsilyl chloride but in the formation of the –siloxane compounds the bonding agent is oxygen while in –silazane case it is nitrogen. Part of the HMDSO reacts with the silanol of the aerogel and is retained in the aerogel product and part of the HMDSO is present in the recovered solvent and can be recycled (Fig. S8).

- Tetraethoxysilane. TEOS is a tetraethoxysilane with the formula $Si(OC_2H_5)_4$. For TEOS preparation many analogues exist, in this process tetraethoxysilane produced from elemental silicon (Si) and ethanol. The GWP for TEOS is calculated according to the chemical composition. Cradle to gate assessment considers raw-material production, transportation and material production. GWP for ethanol and elemental silicon are based on literature [11, 13]: for ethanol 700 g/kg and for elemental silicon 10 000 g/kg. GWP for the production process is taken into account according to information from TEOS producers, where 0.12 kg of CO_2 are generated per kg of TEOS produced. Note that for the 'recycling' case, the ethanol produced by the aerogel production process is recycled back to the TEOS producer.

- Hydrochloric acid and ammonium hydroxide. The LCA data is based on PlasticsEurope data (HCl_u5933 and Ammonia u5835) [14].

As expected, solvent recycling leads to a dramatic decrease of the carbon footprint of the raw materials for silica aerogel production. The use of the one-pot process also decreases the raw materials carbon footprint. The higher carbon footprint of the two-pot process in the case of solvent recycling is mostly related to the energy requirements for purification and the losses on purification (Figure 27).

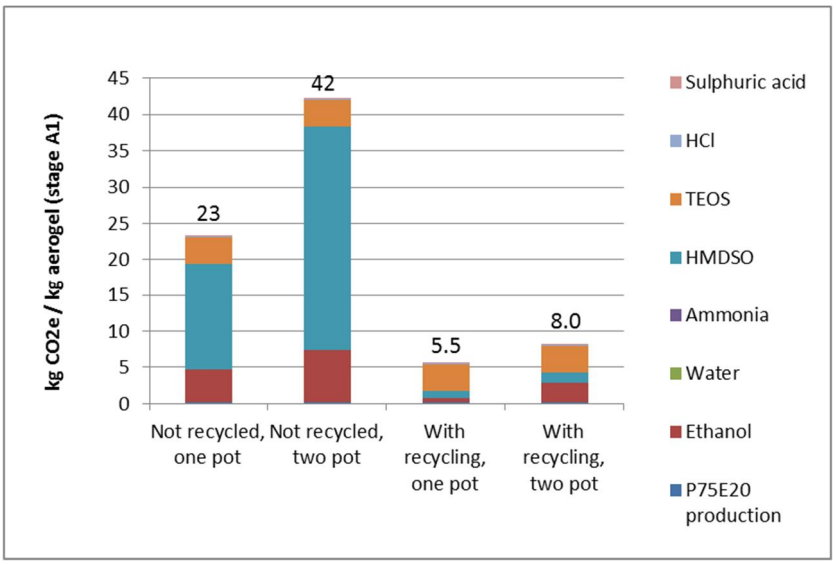

Figure 27. Ambient dried aerogel CO_2e for the life cycle stage: raw-material supply (A1). Aerogel recipes representing one- and two pot production methods for two cases: 1) when aerogel raw-materials are from virgin origin (not recycled) and 2) with a close-loop production and the recycling of HMDSO and ethanol (Figure 14).

CO_2e for raw-material transportation (A2)

Life cycle assessment for aerogel production contains mainly raw-materials which produced in Europe As major TEOS production sites are available in Europe, for example in Antwerp (Belgium) and Rheinfelden (Germany) and as this location might have an impact to the decision for the aerogel production site, transportation distance for TEOS is considered to be small (20 km). HMDSO production sites are available in Germany and a transportation distance of 200 km was selected for HMDSO. The resulting carbon footprint related to raw materials transportation is small: 0.03 and 0.07 kg CO_2e/kg aerogel for the recycling and non-recycling case.

CO_2e for aerogel production (A3)

Aerogel production with ambient drying method contains production phases where elevated heating is used. During the process, waste heat is generated which could be utilized in aerogel production. Recovery of waste heat, from condenser to heat sol/modification solution, is taken into account and it is considered that energy input is needed only for the drying, i.e. going from 90°C up to 150°C. Calculation considers that efficiency in the energy use for the ambient drying process is 50 % and takes into account elevation of temperature, solvent evaporation and drying time. The heating source used for drying is electricity and for the comparison two types of electricity production methods are evaluated: electricity production method with low- and high CO_2e emissions, respectively. CO_2e-values for the electricity with low- and high emissions are respectively 140 g/kWh and 600 g/kWh. The choice of electricity production method has a large effect on the A3 carbon footprint (Figure 28).

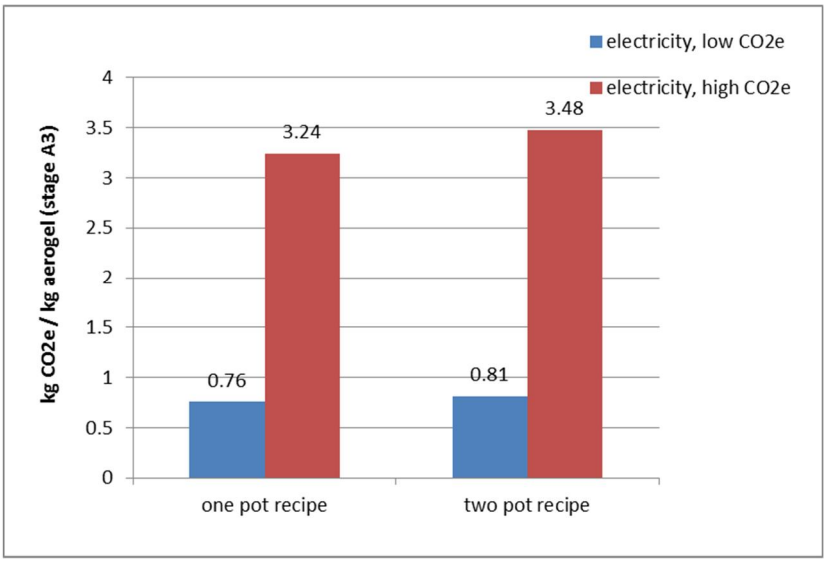

Figure 28. CO_2e from the ambient aerogel production (A3). Production process considers one- and two pot recipes and different electricity sources.

Overall carbon footprint

Life cycle assessment for APD aerogel production stage (A1- A3) is presented in Figure 29 for the one-pot process, with material recycling and electricity used in drying with low or high CO_2e emissions, respectively.

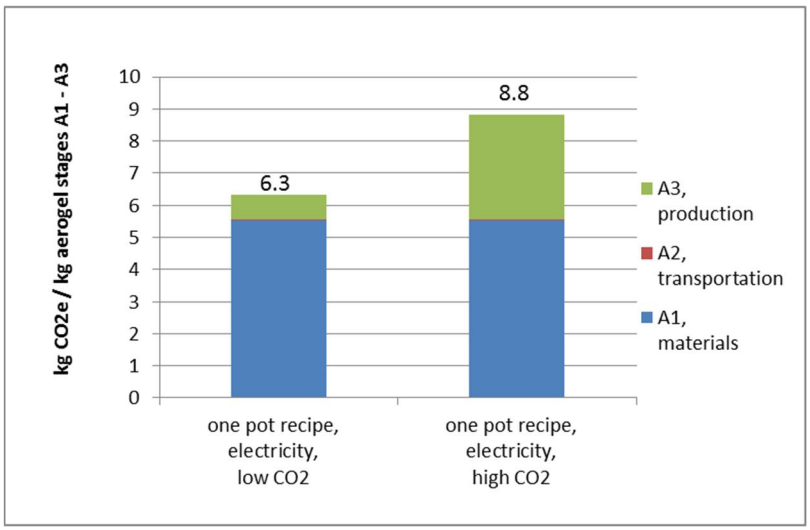

Figure 29. Life cycle assessment for one-pot ambient aerogel production. Assessment contains life cycle stages A1 – A3, for the raw material recycling case and electricity production method with either low or high CO_2e emissions (respectively 140g/kWh and 600 g/kWh).

Task 3.2 Life Cycle Cost

The contribution of APD to the overall production cost is continuously refined in the business cases and plans of Empa and its industrial partner. This information is however confidential. Please contact Dr. Wim Malfait or Dr. Matthias Koebel from Empa for more information.

5. Evaluation of project results

5.1 Work package 1: Fundamental studies on APD

The work on the in situ observation of APD of aerogel materials started well, with the design and construction of a customized heating stage for in situ X-ray microtomography. Multiple proposals for beam-time at the TomCat beamline of the Swiss Light Source (SLS) at the Paul Scherrer Institute (PSI) have been submitted, but were unfortunately declined because insufficient beam-time was available. As a result, these activities cannot be concluded within the current BFE Gelsec project.

The work carried out on APD of pectin-silica hybrid aerogels and polymer-reinforced silica aerogels has clearly demonstrated that APD of these systems is not feasible without a major advance in our understanding of what the requirements are for ambient pressure drying. For all tested drying protocols on these silica hybrids, the APD aerogels were granular materials of relatively high density: in other words: the monolithic gel bodies disintegrated and shrank during APD, despite the use of apolar solvents and despite having tried a range of drying conditions (temperature, solvent partial pressures, etc.). For the (bio)polymer-silica hybrids, the conclusion is thus that APD has not been achieved. In contrast, the APD studies on the cross-linked chitosan aerogels were much more successful, and focus within this part of the project has shifted towards these: the materials prepared with SCD where optimized to a thermal conductivity of 16 mW/(m.K). APD of these systems enabled the production of large monolithic samples (in contrast to silica or silica hybrid aerogels), although the densities were still too high to have a thermal conductivity as low as for the SCD samples. Best performing APD materials have a thermal conductivity below that of standing air, 26 mW/(m.K), and outperform conventional mineral/glass wool and EPS insulation. Hydrophobization was identified as a key step to further increase the performance of the APD materials but this has not been pursued within the current BFE Gelsec project.

Overall, the activities in work package 1 have provided the experimental facilities for in situ observation of APD of aerogels and a new APD aerogel with exceptional properties. However, work on both fronts is incomplete and will be finalized in a follow-up project (see Section 6).

5.2 Work package 2: Optimization and upscaling of APD processes

This workpackage has provided a wealth of data on a wide variety of different drying concepts, including a conical drying under partial vacuum with an integrated condenser, evaporative drying at ambient pressure with a cascade of condensers and finally the development of a new (confidential) drying concept. A series of parameter studies has detailed the role of drying temperature on drying speed and materials quality, both for granulate aerogels and fiber reinforced mats. A second series of parameter studies highlighted the role of gas exchange rate on materials quality, with reduced shrinkage and lower density aerogel produced at high exchange rates. Too high exchange rates however become problematic in terms of condensation efficiency and solvent recovery.

One key observation of this project in terms of solvent recovery was the observation that solvents can be recycled without an additional purification step and this was also confirmed experimentally through the synthesis of aerogels produced from 65% non-purified, recycled solvent. In addition, solvents collected at various steps in the cascade of condensers had remarkably different compositions, which may enable a first separation during condensation. Combined with the reduced need for solvent purification of the Empa one-pot process, this may be sufficient to forego additional solvent purification steps altogether.

The work describe above, and the various drying and condensation concepts tested highlight the difficulties in designing a system that recovers >98% of the solvents with the current oven test-drying

concept. Motivated in part by these unsatisfactory observations, we have designed and implemented a new aerogel drying concept at small scale (1l) for testing and validation purposes. The basic chemical process and material qualities remain the same: the production is still based on the patented, minimal solvent, Empa one-pot process[2, 9] and the materials have thermal conductivities (~18 mW/(m·K) for granulate bed) and densities (0.110 g/cm^3) typical of high quality silica aerogel. The new drying concept reactor was designed from ground up to be gas-tight. Furthermore, because of the higher volume loading of wet gel (wet gel loading in the new system > 20%$_V$ versus ~1.5-2%$_V$ in the convective drying oven system) both solvent and heat recovery is greatly facilitated through the corresponding reduction of carrier gas volume flow. The new concept is currently being implemented at the large pilot scale and will be finalized in a follow-up project (see Section 6).

5.3 Work package 3: LCA of different drying concepts

An extensive, albeit preliminary LCA analysis has been carried out at the start of the project. The LCA analysis concludes that processing, including APD, has only a very minor contribution to the overall CO_2e emissions and embodied energy, provided low CO_2e electricity is used to energize the APD, which is possible thanks to the particular nature of the Swiss electricity production. Raw materials account for the vast majority of the CO_2e emissions, but these are also lower thanks to Empa one-pot technology. Overall, the LCA confirms the benefits of aerogel production through the Empa process combined with APD.

5.4 Overall evaluation

This BFE project was overall successful in attaining the project goals set out at the start.

The fundamental studies are well underway: new exciting instrumentation was constructed and new APD biopolymer aerogels developed. The work on both of these topics has not been concluded, but financing has been obtained to carry these activities through to fruition (see Section 6). As such, this BFE project has initiated activities that have to potential to limit energy consumption through sustainable aerogel insulation on the long term.

The second and major aim of this project has shorter timelines. Here, the project's major success lies in the evaluation and optimization of various drying concepts that culminated in the development of a new concept that ensures a high solvent recovery rate. This concept was implemented successfully at the 1 liter scale and is now being implemented at the much larger scale in a follow-up project (see Section 6). LCA of the production process confirms the energy efficiency and limited CO_2e emissions of the chosen production route. As such, the project really has provided an important step towards the mass production of silica aerogels through ambient pressure drying.

6. Outlook and next steps

The successful activities in this BFE-GELSEC project have enabled us to secure financing for the follow-up activities.

Concerning the more fundamental studies and biopolymer aerogels, the Swiss National Science Foundation recently granted a project to our laboratory (SNF 200021_179000, Biopolymer Aerogels for Thermal Superinsulation 01.05.2018-31.04.2022). The abstract of the project is as follows:

Aerogels are highly porous, mesoporous solids with a range of exceptional properties, such as high surface area, high strength-to-weight ratio, and low thermal conductivity. Thanks to its ultra-low thermal conductivity, silica aerogel insulation has grown into a global market of ~300 Mio CHF during the last decade. Further innovations and new silica aerogel production processes, developed within my group and undergoing commercialization will further accelerate this growth. Biopolymer aerogels are derived from renewable feedstocks, but do not exhibit the scientific maturity, market size or production volume of silica aerogel, despite ongoing academic research and a large potential for thermal superinsulation. The overarching aims of this project are to advance biopolymer aerogels for thermal insulation through a fundamental understanding of chemistry-structure-property relations, to develop new hydrophobization and crosslinking strategies, and to enable ambient pressure drying (APD) of selected biopolymer aerogel systems. We focus on chitosan aerogels produced with a non-isocyanate route. First, the reaction will be optimized both in the presence and absence of catalysts. Then, chitosan aerogels with high surface area and low thermal conductivity will be synthesized by supercritical CO_2 as well as APD, a unique feat for biopolymer aerogels. The reaction optimization will be supported by in situ NMR spectroscopy and the APD optimization by in situ X-ray microtomography. We will determine the factors that govern the microstructure of biopolymer-silica aerogels by systematic parameter studies of biopolymer chain length and functionality and the synthesis parameters (temperature, pH). The molecular interactions and structure of selected samples will be analysed by advanced analytical techniques such as solid-state NMR and infrared spectroscopy with nm scale resolution (AFM-IR). Finally, new strategies will be developed to hydrophobize polysaccharide aerogels and the resulting materials will be subjected to accelerated aging.

Concerning the pilot production of silica aerogel through ambient pressure drying, BFE provides partial funding for a BFE P&D project to be carried out in our laboratory (BFE P&D SI/501607-01, Pilot scale optimization for cost- and energy-effective silica aerogel production using a disruptive chemical process, 16.09.2017-15.09.2019). The project abstract is the following:

Aerogel requires half the insulation thickness for the same thermal performance, are non-flammable and water vapour open, and ideal for retrofitting and indoor applications. We developed a cost- and energy-efficient production route for silica aerogel and demonstrated proof-of-concept at the 40l pilot scale. During and after this P&D project, the technology will be transferred to industry. An additional pilot study closer to an industrially scalable concept is needed before the investments for a production line can be justified. With these last technological refinements in place, this manufacturing technology will cut the price of silica aerogel in half, enabling the transition from niche to mass markets. This will generate energy savings through improved thermal insulation, particularly in cases where space is limited and no cost-competitive solutions are available today.

Combined, these follow-up projects guarantee that the project results will be carried forward and brought closer to scientific maturity and industrial implementation.

7. References

[1] M. A. Aegerter, N. Leventis, M. M. Koebel, *Aerogels Handbook*, Spriner-Verlag, New York, **2011**.

[2] aL. Huber, S. Zhao, W. J. Malfait, S. Vares, M. M. Koebel, *Angewandte Chemie International Edition* **2017**, *57*, 4753-4756; bM. M. Koebel, L. Huber, S. Zhao, W. J. Malfait, *Journal of Sol-Gel Science and Technology* **2016**, *79*, 308-318.

[3] aS. Zhao, W. J. Malfait, A. Demilecamps, Y. Zhang, S. Brunner, L. Huber, P. Tingaut, A. Rigacci, T. Budtova, M. M. Koebel, *Angewandte Chemie International Edition* **2015**, *127*, 14490-11494; bS. Zhao, W. J. Malfait, E. Jeong, B. Fischer, Y. Zhang, H. Xu, E. Angelica, W. M. Risen, J. W. Suggs, M. M. Koebel, *ACS Sustainable Chemistry and Engineering* **2016**, *4*, 5674-5683; cS. Zhao, Z. Zhang, G. Sebe, R. Wu, R. V. R. Virtudazo, P. Tingaut, M. M. Koebel, *Advance Functional Materials* **2015**, *25*, 2323-2334.

[4] S. Brunauer, P. H. Emmett, E. Teller, *J. Am. Chem. Soc.* **1938**, *60*, 309-319.

[5] E. P. Barrett, L. G. Joyner, P. P. Halenda, *J. Am. Chem. Soc.* **1951**, *73*, 373-380.

[6] G. Reichenauer, in *Aerogels Handbook* (Eds.: M. A. Aegerter, N. Leventis, M. M. Koebel), Springer, New York, **2011**, pp. 449-498.

[7] aT. Stahl, S. Brunner, M. Zimmerman, G. W. K., *Energy and Buildings* **2012**, *44*, 114-117; bJ. C. H. Wong, H. Kaymak, S. Brunner, M. M. Koebel, *Micropor. Mesopor. Mat.* **2014**, *183*, 23-29.

[8] S. Iswar, G. M. B. F. Snellings, S. Zhao, R. Erni, Y. K. Bahk, J. Wang, M. Lattuada, M. M. Koebel, W. J. Malfait, *Acta Materialia* **(submitted)**.

[9] M. M. Koebel, S. Zhao, S. Brunner, C. Simmen, **2015**.

[10] L. M. Vane, F. R. Alvarez, *Journal of Chemical Technology and Biotechnology* **2008**, *83*, 1275-1287.

[11] I. Muños, K. Flury, N. Jungbluth, G. Rigarlsford, I. Mila, L. Canals, H. King, *International Journal of Life Cycle Assessment* **2014**, *19*, 109-119.

[12] J. Sutter, *Ecoinvent report nr. 19* **2007**.

[13] B. Brandt, E. Kletzer, D. Hadzhiyska, P. Seizov.